Arch. Metall. Mater. **68** (2023), 2, 711-722

DOI: https://doi.org/10.24425/amm.2023.142453

M.R. HAWRYLUK[1], M. LACHOWICZ[1], M. JANIK[1*], Z. GRONOSTAJSKI[1], M. STACHOWICZ[1]

EFFECT OF THE HEATING TEMPERATURE OF A NICKEL-CHROMIUM STEEL CHARGE MATERIAL ON THE STABILITY OF THE FORGING PROCESS AND THE DURABILITY OF THE DIE

The study discusses the issues of low durability of dies used in the first operation of producing a valve type forging from high nickel steel assigned for the application in motor truck engines. The analyzed process of manufacturing the exhaust valve forgings is realized in the coextrusion technology, followed by forging in closed dies. This process is difficult to master, mainly due to elevated adhesion of the charge material (high nickel steel – NCF3015) to the tool substrate as well as very high abrasive wear of the tool, most probably caused by the dissolution of hard carbide precipitates during the charge heating. A big temperature scatter of the charge during the heating and its short presence in the inductor prevents microstructure homogenization of the bearing roller and dissolution of hard precipitates. In effect, this causes an increase of the forging force and the pressures in the contact, which, in extreme cases, is the cause of the blocking of the forging already at the beginning of the process. In order to analyze this issue, complex investigations were conducted, which included: numerical modelling, dilatometric tests and hardness measurements. The microstructure examinations after the heating process pointed to lack of structure repeatability; the dilatometric tests determined the phase transformations, and the FEM results enabled an analysis of the process for different charge hardness values. On the basis of the conducted analyzes, it was found that the batch material heating process was not repeatable, because the collected samples showed a different amount of dissolved carbides in the microstructure, which translated into different hardnesses (from over 300 HV to 192 HV). Also, the results of numerical modeling showed that lower charge temperature translates into greater forces (by about 100 kN) and normal stresses (1000 MPa for the nominal process and 1500 MPa for a harder charge) and equivalent stresses in the tools (respectively: 1300 MPa and over 1800 MPa), as well as abrasive wear (3000 MPa mm; 4500 MPa mm). The obtained results determined the directions of further studies aiming at improvement of the production process and thus increase of tool durability.

Keywords: forging; engine; chromium-nickel steel with austenitic microstructure; valve; forging tools

1. Introduction

The suction and exhaust valves in combustion engines of motor trucks and tractors operate at the temperatures of 600-800°C [1]. The high pressure values inside the engine chamber exceeding 200 MPa cause cyclic thermal and mechanical pressures onto the valves, which makes the material they are made of the key aspect [2,3]. Engine valves are usually produced in the process of hot plastic treatment from high nickel austenitic steels or a nickel superalloy (about 80% Ni), which characterize in high corrosion resistance in combustion gases, hardness abrasion resistance at high temperatures and high temperature creep resistance [4].

At present, in the valve production processes, the applied technology is based on a process of forging in closed dies consisting of two operations: hot extrusion of a long shank tipped with a preliminarily formed element called "pear" and next finishing forging of the valve head. Despite the fact that this technology is difficult to master, it makes it possible to obtain products (forgings) characterizing in better mechanical properties and surface quality (high performance properties) [5,6].

Currently, the most frequently applied material for the production of valves according to the second technology are nickel alloys type Nimonic 80A [7]. In the global literature, there are a few studies devoted to the forging of this alloy, which, however, mainly refer to the microstructural changes taking place during their deformation [8,9]. We can also find works discussing the issue of tool durability [10]. Nickel alloys characterize in high creep resistance and corrosion resistance at high temperatures, which is conditioned by their precipitation-hardened microstructure [11,12]. The microstructure of these alloys consists of a solid solution γ and precipitates of phase γ' coherent with

[1] WROCŁAW UNIVERSITY OF SCIENCE AND TECHNOLOGU, FACULTY OF MECHANICAL ENGINEERING, 5 IGNACEGO ŁUKASIEWICZA STR., 50-371 WROCŁAW, POLAND

* Corresponding author:marta.janik@mahle.com

the matrix, which are constituted by the intermetallic phase $Ni_3(Al,Ti,Nb)$ [13,14]. The high price of nickel enforces the necessity of searching for other replacements of this steel, hence the attempts at introducing chromium-nickel steels [15]. One of the representatives of this group of materials is steel commercially named Nireva, known also as NCF 3015, which nominally contains 30% nickel and 15% chromium. Alloys with such a chemical composition in the as-delivered state consist of an austenitic matrix and carbide precipitates distributed inside the grains as well as on their boundaries. The presence of a chromium content is a factor which contributes to the formation of oxide layers, which translates to a high heat resistance of this alloys. It increases with the chromium and nickel content in the steel. A long term operation at high temperatures contributes to the formation of complex oxide layers [16]. The literature data points to the fact that, in alloys from the Ni-Cr-Fe system, carbides type MC, M_6C and $M_{23}C6$ mostly precipitate [17]. MC type carbides precipitate during solidification as a result of carbon segregation. They are distributed in the form of regular precipitates localized inside the grains. Carbides of this type are formed by carbon mainly with titanium, niobium and molybdenum. They are stable even at high temperatures; however, they have a tendency for decomposition into complex carbides. $M_{23}C_6$ type carbides are formed mainly by chromium and localized on the grain boundaries. The temperature scope of the chromium carbide formation is determined between 550°C and 1050ºC [17], where the highest intensity of precipitation is observed in the vicinity of 850°C. The formation of carbides on the grain boundaries has also been observed in nickel alloys during heating to high temperatures and slow cooling [18]. $M_{23}C_6$ carbide obviously lowers the strength of the steel when it precipitates along the grain boundaries [19]. On the one hand, their presence on the grain boundaries favours the increase of the creep resistance as well as blocking of the austenite grain growth. On the other hand, however, it significantly lowers the material's ductility as well as hinders the forging process by lowering the tool durability. The formation of chromium carbides on the gain boundaries leads also to the formation of chromium depleted zones, which lowers their intergranular corrosion. At the same time, the presence of carbides on the grain boundaries improves the stress corrosion by limiting the possibility of crack propagation. Ageing of alloy NCF 3015 after supersaturation, similarly to the case of nickel alloys, leads to precipitation of fine precipitates which reinforce the alloy. A properly performed thermal treatment aims at supersaturation conducted at 1050°C, followed by ageing at 750°C performed for 4 hrs [20].

The biggest problem in the forging processes are very high pressures, which translate to lowered die durability (in extreme cases, even a dozen or so forgings) and the formation of faulty products resulting from the difficulty in forming steel with a high nickel content and the selection of optimal process parameters [21,22]. We can often observe an increased adhesion of the charge material made of chromium-nickel steel (25-35% nickel and about 15-20% chromium) to the substrate of a tool made of typical tool steel (e.g.: W360 or WLV) during the hot coextrusion process [23,24]. As a result of high pressures and temperatures, as well as a long path of friction, we observe blocking of the extruded material in the die's eye. Additionally, another occurring problem is the lack of stability of the charge material heating process. It is so because, in the case of steel NFC3015, with a relatively low heating temperature in the last phase (1040°C), the hard precipitates do not dissolve in the preform, which results in its increased hardness. In consequence, it causes higher forming forces and higher pressures, which lead to premature wear and blocking of the die in the impression. And so, in the case of steels used as the charge for the production of valve forgings, it is also important to control and stabilize the heating, and it is sometimes even necessary to heat the charge for a short time in order to dissolve the hard particles.

At present, for the heating of the charge, induction heating is applied, which ensures fast heating times correlated with the production cycle. The charge material heating processes for the die forging are being constantly improved and still constitute a challenge in the scientific, technological and economical aspect [25,26]. One of the most frequent methods of heating to a specific temperature in die forging and extrusion processes is induction heating, which has a big advantage over other alternative charge heating methods [27]. The main problem to be solved during the charge heating are undoubtedly the oxidation and decarburization of the charge surface, which has its consequences in the quality of the produced forging. Moreover, for economic reasons, the production cycle has to be very short, which, in extreme cases, prevents the possibility of total dissolution of the hard carbides. The current technologies with the use of induction heating, in terms of solutions for the heating system itself, are based on devices equipped with sector inductors, with the possibility to regulate the voltage and the travel speed in the heating section, which makes the temperature gradient of each section changeable [28]. The most frequent solution is dividing the heating section of the induction heater into three or more parts, depending on the size of the device [29]. Currently, the most advanced technologies enabling an even bigger universality of the induction heater, in respect of the constant frequency inductors, is the application of varying frequency inductors [30].

The low durability of tools made of tool steels for hot operations is the main problem in the case of forming forgings from austenitic steels, and this currently constitutes a difficult and still unresolved problem, which is a big challenge for scientists from the field of materials engineering as well as technologists of processes such as die forging. It is of key importance to select the proper technological parameters, such as tribological conditions, including lubrication, the optimal shape of the forming tools ensuring reduced forming forces as well as minimized residual deformations [31,32].

The relatively low durability of tools used to produce valves is a consequence of the presence, with different frequencies, of many destructing phenomena and mechanisms. The most important ones include: abrasive wear, thermo-mechanical fatigue, plastic deformation, fatigue cracking as well as adhesive wear and oxidation. This, in combination with cyclic thermo-

mechanical loads to which the forging tools are exposed, as well as the dynamics and instability of the forging process, makes the forging processes one of the most difficult to realize and analyze. The key aspect is also the dissolution of the hard carbide precipitates during the charge heating, which often causes premature wear of the forging tools (dies). And so, it is justifiable to perform advanced complex studies enabling an analysis of the destructive phenomena and mechanisms, especially investigations and analyses of the microstructure of the charge material and the dies. On this basis, it will be possible to undertake reparatory and preventive measures as well as propose methods enabling an increase of the forging tool durability [33-35]. This, in turn, will reduce the costs per unit of the production of valve type forgings as well as other elements manufactured in die forging processes from high nickel austenitic steels, for which the mean durability is much lower than for carbon steels.

2. Materials and methods

A detailed analysis was performed on dies used in I operation of hot coextrusion of a long shank ended with a preliminarily formed element called "pear", for which, in the case of the hard precipitates not being sufficiently dissolved in the heated material, blocking or rapid damage occurred (Fig. 1).

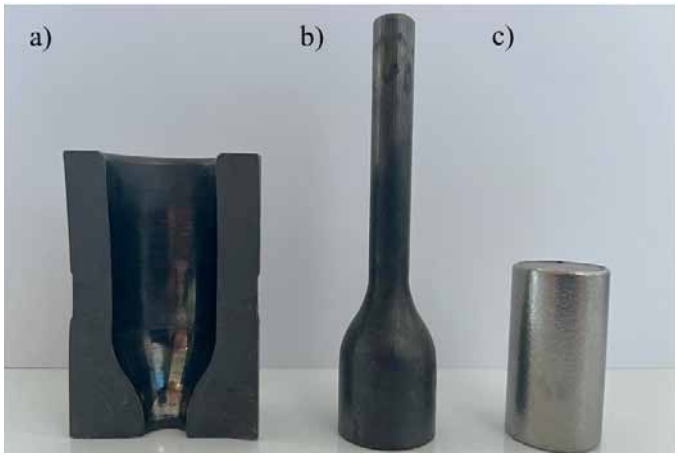

Fig. 1. View of: a) tool section, b) „pear", c) charge material

The dies are made of hot operation tool steel QRO90, subjected to thermal treatment and next gas nitriding. The impression surface of the ready tools characterizes in hardness of about 1100HV. The ready tools are heated to the working temperature of about 200°C and mounted in the press. The temperature of the charge material equals 1040°C. During the extrusion process, the tools are lubricated and cooled with a cooling and lubricating agent based on graphite. The mean die durability is about 1000 items. A detailed analysis was made of a series of bearing rollers after the heating and before the extrusion. The inductor length after the heating equals 680 mm, and the mean time of the charge's presence in the inductor is over 100 sec. The bearing rollers, after exiting the inductor, were cooled with water.

During the analysis, the following research techniques were applied:

– FEM modelling of the tool operation under different friction and temperature conditions performed in the Forge3.0 program;
– a chemical analysis of the Nireva material, carried out with the use of the LECO 750-GDS-QDP spectrometer (LECO Corporation, St. Joseph, MI, USA) with a glow discharge in an argon shield;
– microscopic tests by means of a scanning microscope PhenomProX coupled with an EDX detector;
– a direct dilatometer Linseis L75 HS;
– examinations of the charge material microstructures after etching in a 10% oxalic acid solution;
– a hardness measurement with a LECO hardness tester.

3. Results and discussion

To make the deep problem analysis, there were several complex researches performed, e.g. numerical analysis, chemical composition as well as microstructure and dilatometric checks. Based on that, there was a trial to simulate the heating system of charging material, to ensure the possibility of correct heating and dissolution of hard phases.

3.1. Analyze of Finite Element Modeling

For a more thorough analysis, numerical modelling was conducted of I operation for two variants. The first one is a nominal process, for which, with the charge temperature of 1040°C, the hardness was at the level of 230 HV. In the second variant, the assumed charge temperature was lower by 100°C, and thus the charge material hardness was about 300 HV. The simulations were carried out in order to compare the selected key parameters deciding about the tool durability (von Misses reduced stresses, normal stresses, path of friction and forging forces). In the numerical simulations of the valve forging, an axisymmetric model with deformable tools was applied in the Forge 3.0 Nxt program. The material for the tools (steel W360 ISOBLOC – BÖHLER) were assumed from the program database. As the forging material, steel 1.4981 (X8CrNiMoNb16-16) was used, which had the chemical composition for the analyzed chromium-nickel steel (NCF3015). Fig. 2 shows a general view of the model before and after the simulation of I forging operation.

For the simulation, the data based on the industrial process were assumed, presented below:

- Temperatures: charge – 1040°C, tools – 200°C, environment – 30°C;
- Press: Metal Pres 700 E;
- Friction model according to Tresca: $f = 0.4$;
- Thermal conductivity in the contact – 10 kW/m²×K (denoted as the medium in the program);

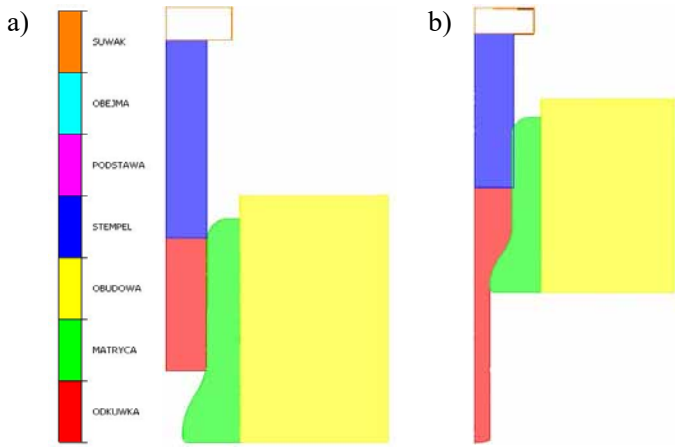

Fig. 2. A general view of the model: a) before, b) after I forging operation

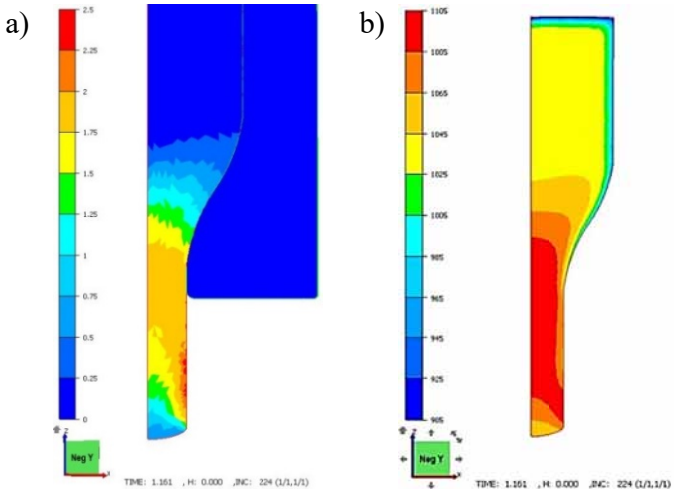

Fig. 3. Distributions on the forging at the last forging stage: a) deformations and b) temperatures

- Thermal conductivity with the environment – 15 W/m² × K (determined experimentally);
- Contact time of the preform with the die before the stroke – 1.5 s;
- Charge hardness for the nominal process 220 HV – for the second variant corresponding to lack of dissolution of the hard precipitates, the assumed hardness was at the level of 300 HV.

Fig. 3 shows exemplary distributions of deformations and temperatures on the forging at the last forging stage. Based on the obtained results, we can observe that the biggest deformations occur in the "leg" of the forging and equal about 2. The case was similar of the temperature distributions, whereas, we can see that, as a result of mostly the change of the deformation work into heat and friction, in the vicinity of the forging leg, the temperature increased from the initial 1040°C by about 60°C to 1100°C. In turn, in the non-deformed or slightly deformed area, as a result of contact with the cooler tools, the temperature was lowered right at the surface even to as much as about 900°C.

Fig. 4 presents a comparison of the reduced stress distributions at the beginning and end of the process for both variants.

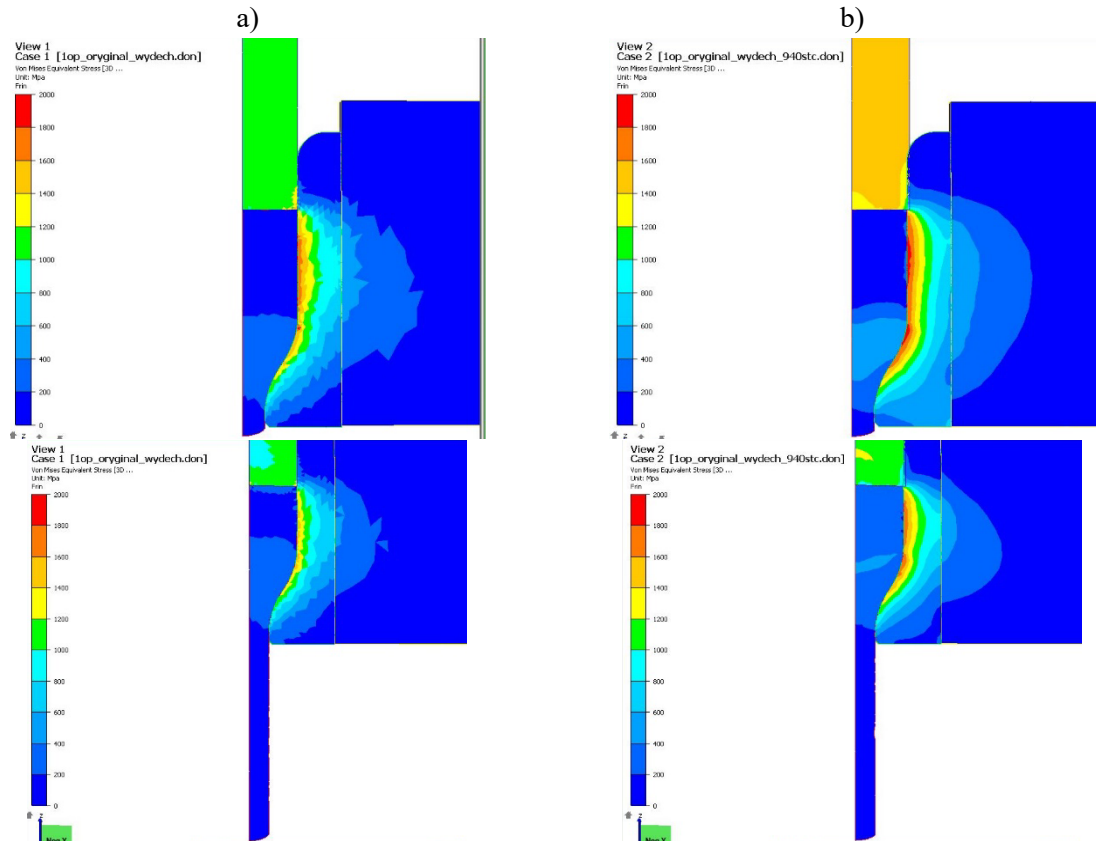

Fig. 4. Distributions of reduced stresses in the die at the beginning and end of the forging process in I operation: a) nominal variant, b) for a higher charge hardness

Analyzing the results for both variants, we can notice that the highest values occur in two areas: the upper cylindrical part of the die and the degree of reduction of the forging section area, where much higher stress values are present for a higher hardness of the charge, which reach almost 2000 MPa, while, for the nominal process, they reach about 1600 MPa. In turn, in the last process phase, for both cases, the stresses are lower, while being still higher, and equal: 1200 MPa in the nominal process and in the process with a higher charge hardness.

Fig. 5 shows a comparison of the normal stress distributions for both variants and at the end of the forging process.

The unit stress distributions shown in Fig. 5 present themselves similarly to the von Misses reduced stresses, where, in the case of the formation beginning, high stresses are present on the cylindrical walls of the die for a higher charge material hardness, while, in the part of the die with a reduction of the section area, the pressures for both cases are the same and equal about 1800 MPa. Towards the end of the forging process, the situation is analogical, with the pressures being slightly lower. The higher values in the cylindrical part of the die for a harder charge can be caused by a reaction activated by the fact that the first contact of the charge with the die takes place on the conical part of the tool, where the diameter is smaller than that of the charge, which translates to increased pressures in the cylindrical part for the harder charge material.

Fig. 6 shows the abrasive wear distributions in the final phase of the forging process for both cases.

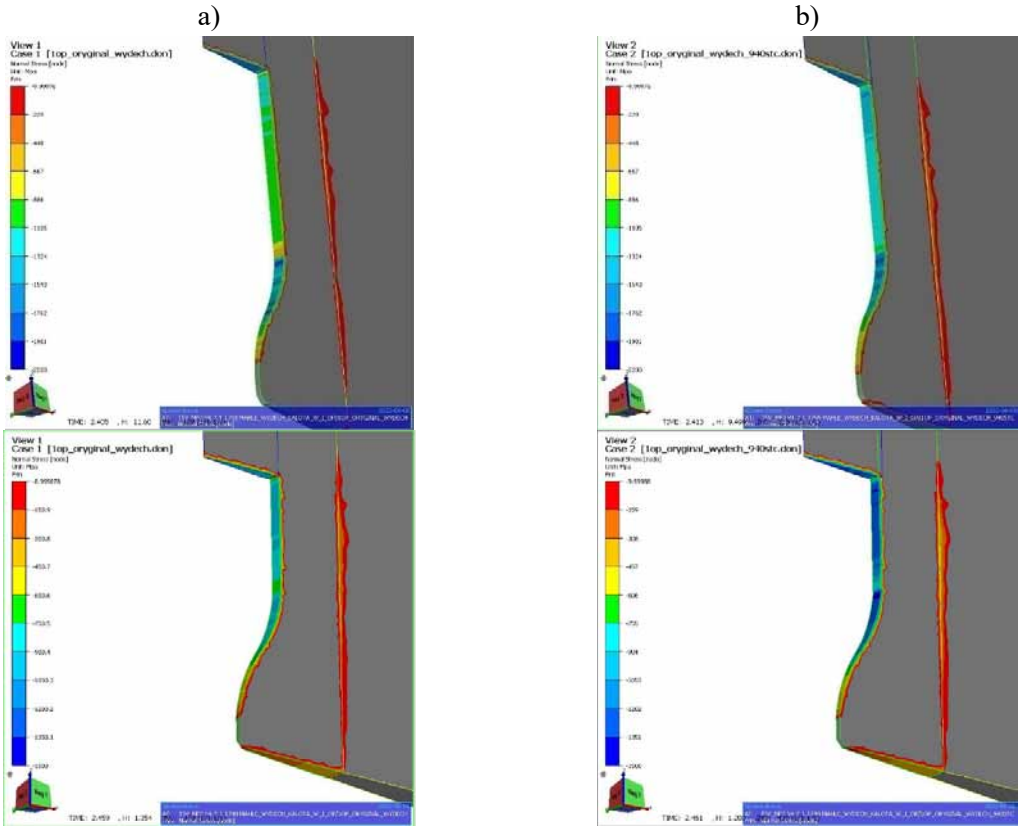

Fig. 5. Unit stress distributions in the die at the beginning and end of the forging process in I operation: a) nominal variant, b) for a higher charge hardness

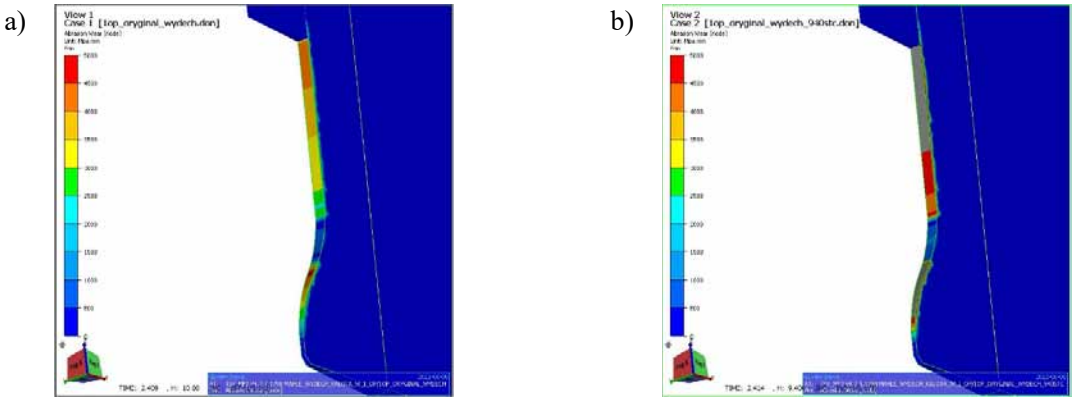

Fig. 6. Distributions of abrasive wear in the die at the end of the forging process in I operation: a) nominal variant, b) for a higher charge hardness

As we can notice, higher values of abrasive wear occur for the harder charge material, and the highest ones, equaling over 4500 MPa mm, are localized in the transition zone of the die at the beginning of the section area reduction. The obtained results point to the possibility of blocking of the forging material in this area, especially for a harder charge material.

Fig. 7 presents the courses of the forging forces in I operation in the function of time for both analyzed variants.

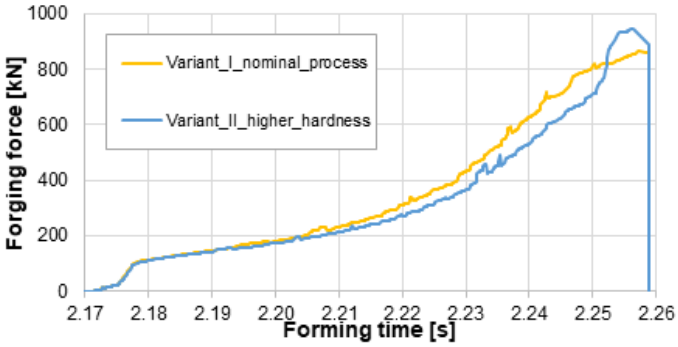

Fig. 7. Forging force courses in I operation for both analyzed variants (nominal and with an increased charge hardness)

The obtained courses suggest that, in the case of the harder charge material, the maximal force values are higher by about 100 kN. What is more, the force increases more rapidly in the last forming phase. In paper [36], the authors, conducting numerical modeling, noticed changes in the grain size for a similar material forging in closed dies in the temperature range of 950-1250°C, which may also affect the amount of carbides. Similarity in works [37,38] numerical modeling was used to forecast grain size in relation to temperature or cooling rate, deformation heterogeneity in the deformed material at high temperatures.

The obtained FEM results point to the fact that, in the case of the harder charge material, the selected physical quantities based on which we can conclude about the die durability are higher in respect of the nominal process, which can be the cause of premature wear of the die or blocking of the forging inside it, thus disqualifying such a tool from further operation.

3.2. Chemical composition determination

TABLE 1 presents the chemical composition determined by means of a spectrometer LECO 750-GDS. The NCF3015 material characterizes in a very high content of chromium and nickel. The numerous alloy additions (Al, Ti, Nb) form intermetallic phases as well as carbides and nitrides. Received chemical composition results for analysed material are according to the material specification.

3.3. Microstructural tests

Researches have been divided into two steps: 1st step Related with material coming from ironwork, 2nd step Related with verification of charging material after heating.

3.3.1. Tests of material as-delivered

In the as-delievered state, a very fine-grained austenitic microstructure with carbide precipitates forming a continuous halo on the grain boundaries was established. Also, two types of precipitates were observed – with bigger dimensions distributed in the austenitic matrix, with a grey and orange colouring. The surface element distributions obtained from such exemplary precipitates have been presented in Figs. 8 and 9. On their basis, it was established that they were constituted by precipitates of large primary alloy carbides (Ti,Nb,Mo,Zr)C as well as titanium nitrides, respectively. The microscopic observations demonstrated that the nitride precipitates can form a crystallization base for alloy carbide precipitates, which proves their higher crystallization temperature (Fig. 10). The material hardness in

TABLE 1

Chemical composition of the forging material (NCF3015)

Element	C	Si	Mn	Ti	Ni	Mo	Al	Cr	Nb	Cu	V
NCF3015	0.04	0.25	0.43	2.69	32.20	0.61	1.61	14.16	0.46	0.02	0.05

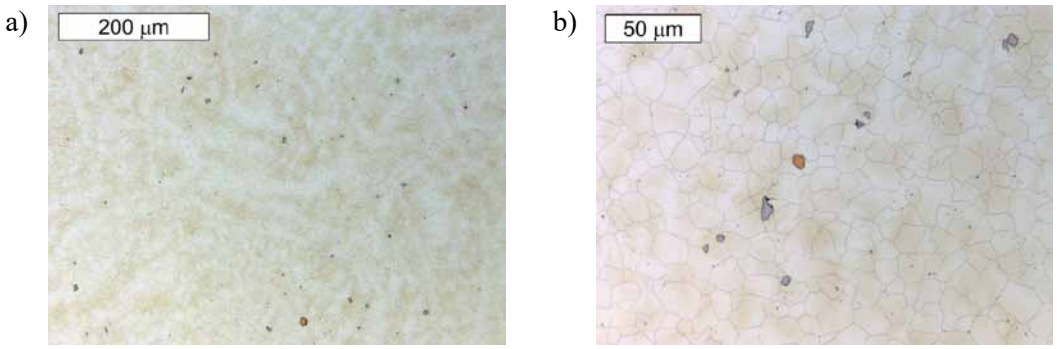

Fig. 8. Microstructure of Nireva as-delivered. Light microscopy, etched

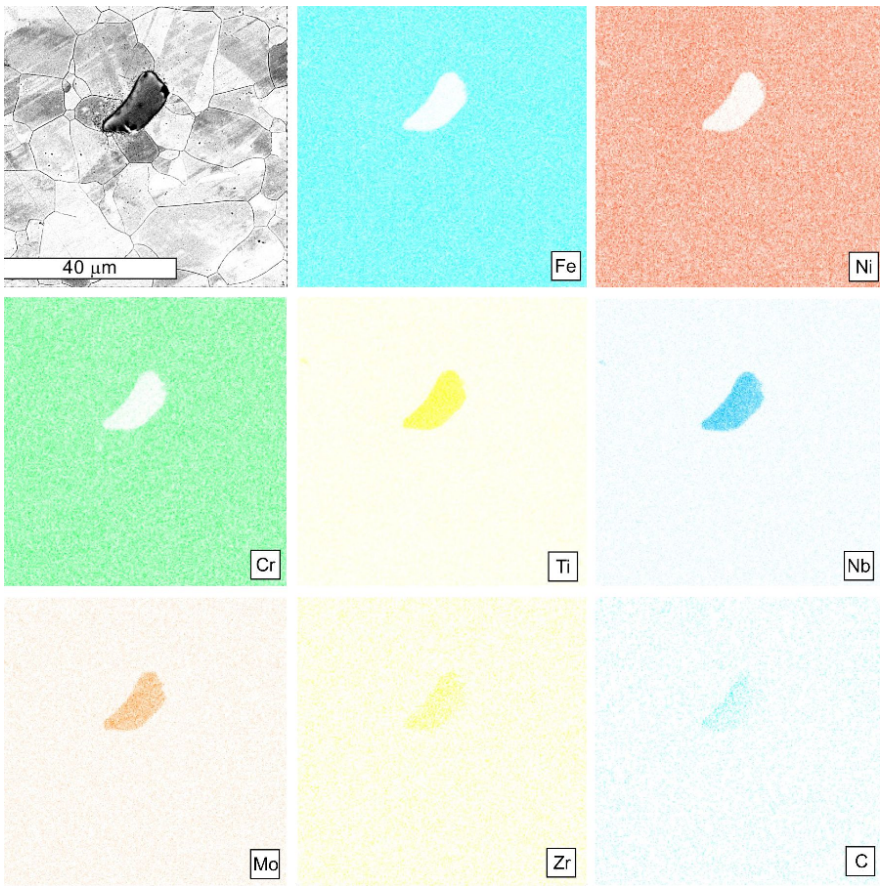

Fig. 9. Surface element distribution obtained from an exemplary precipitate observed in the microstructure of the Nireva material. FEM/EDS

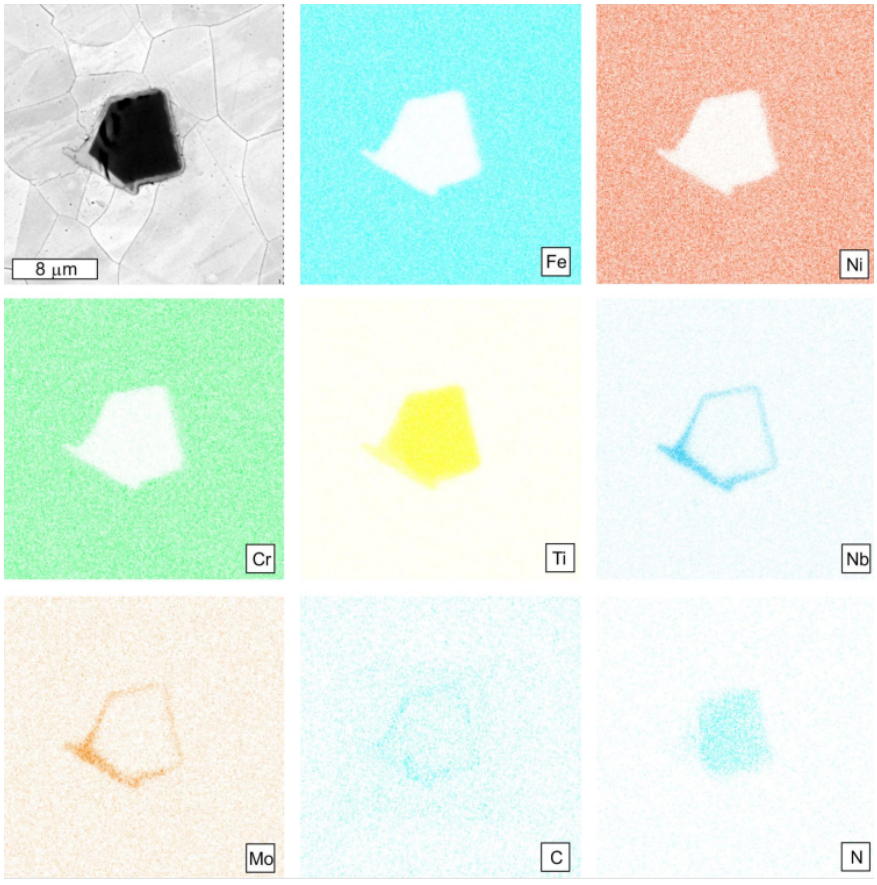

Fig. 10. Element surface distribution obtained from an exemplary precipitate observed in the microstructure of the Nireva material. FEM/EDS

the as-delivered state equaled 351±7 HV1. The presence of high-stability primary carbide precipitates in alloys with high nickel content was also observed by other authors [39].

3.3.2. Tests of material after heating

At the following stage of studies, tests of nine samples were performed after one-time induction heating followed by cooling in water. The test samples were collected randomly at distances of 100 items. The microstructure images of the materials with the highest and lowest obtained hardness have been shown in Figs. 11 and 12. The microstructure of the other seven preforms have been shown at large magnifications in Fig. 13 according to the decreasing hardness values. As a result of the performed investigations, it was established that the samples after the one-time heating combined with the following supersaturation demonstrate a significant variability in the obtained hardness values, which is connected with different degrees of dissolution of the carbide precipitates present on the grain boundaries. The presence of precipitates distributed along the grain boundaries is related to the high density of dislocations occurring in this area [40]. Precipitates should dissolve in the matrix during heating, and the following rapid cooling rate inhibits their re-precipitation. Despite the maintained same parameters, not each sample obtained dissolution of carbide precipitates present on the boundaries of the austenite grains. This indicates that the solutioning process has not been completely completed while heating. In the same way, the material after saturation demonstrated a varying hardness equaling from 192 to as much as 333 HV10. The presence of carbides promotes higher hardness, and the increase in this hardness depends on the type and content of carbides [41,42]. The microscopic observations clearly show the higher the material hardness, the higher the content of the carbide precipitate on the austenite grains. In the case of the material with the highest hardness, it was possible to observe segregation of the chemical composition, typical of an as-delivered material. It was established that this can be affected by two factors, i.e. too short heating time or the changeability of the heating temperature. However, the obtaining of properly supersaturated microstructures with the same heating time suggests that the key importance in this respect is probably that of the temperature variability. This will translate to tool material durability, as the harder the material, the shorter the tool operation time. A frequent phenomenon occurring during extrusion from an underheated material is the problem with the initiation of the extrusion process: at the first stage, the forging is blocked in the tool, which makes it impossible to continue the forming process. For this reason, proper dissolution of carbides will stop the homogenized microstructure from significantly affecting the tool durability.

3.4. Dilatometric studies

For a precise determination of the temperaturre scope in which we observe dissolution of the phases occurring on the grain boundaries in the austenite, dilatometric tests were conducted for two steel suppliers (2 samples for each supplier, dimensions

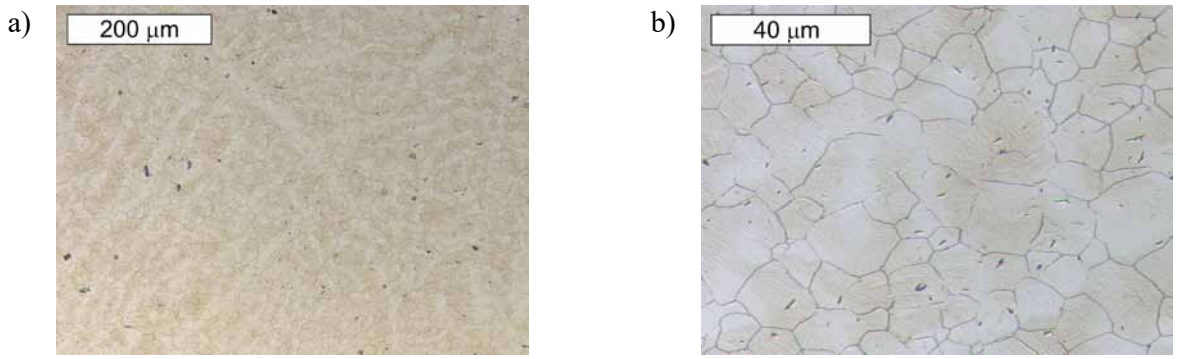

Fig. 11. Material microstructure with the hardness after heating of 333 HV10 (sample H). Light microscopy, etched

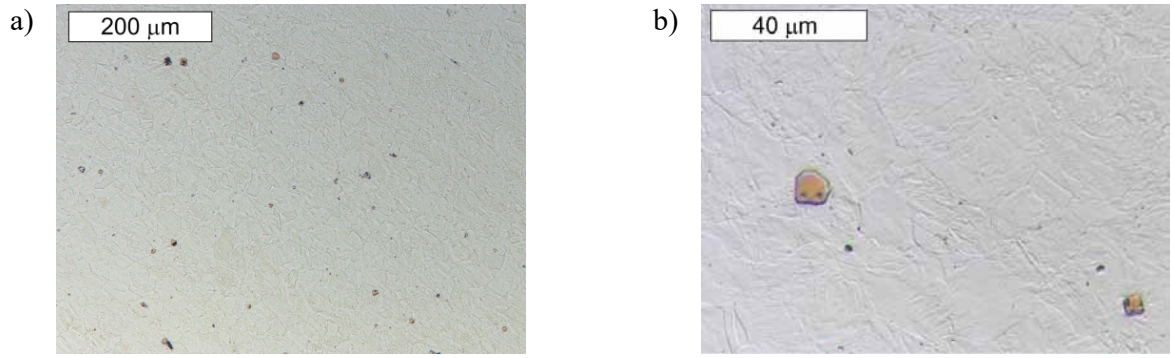

Fig. 12. Microstructure of the material with the hardness after heating of 192 HV10 (sample E). Light microscopy, etched

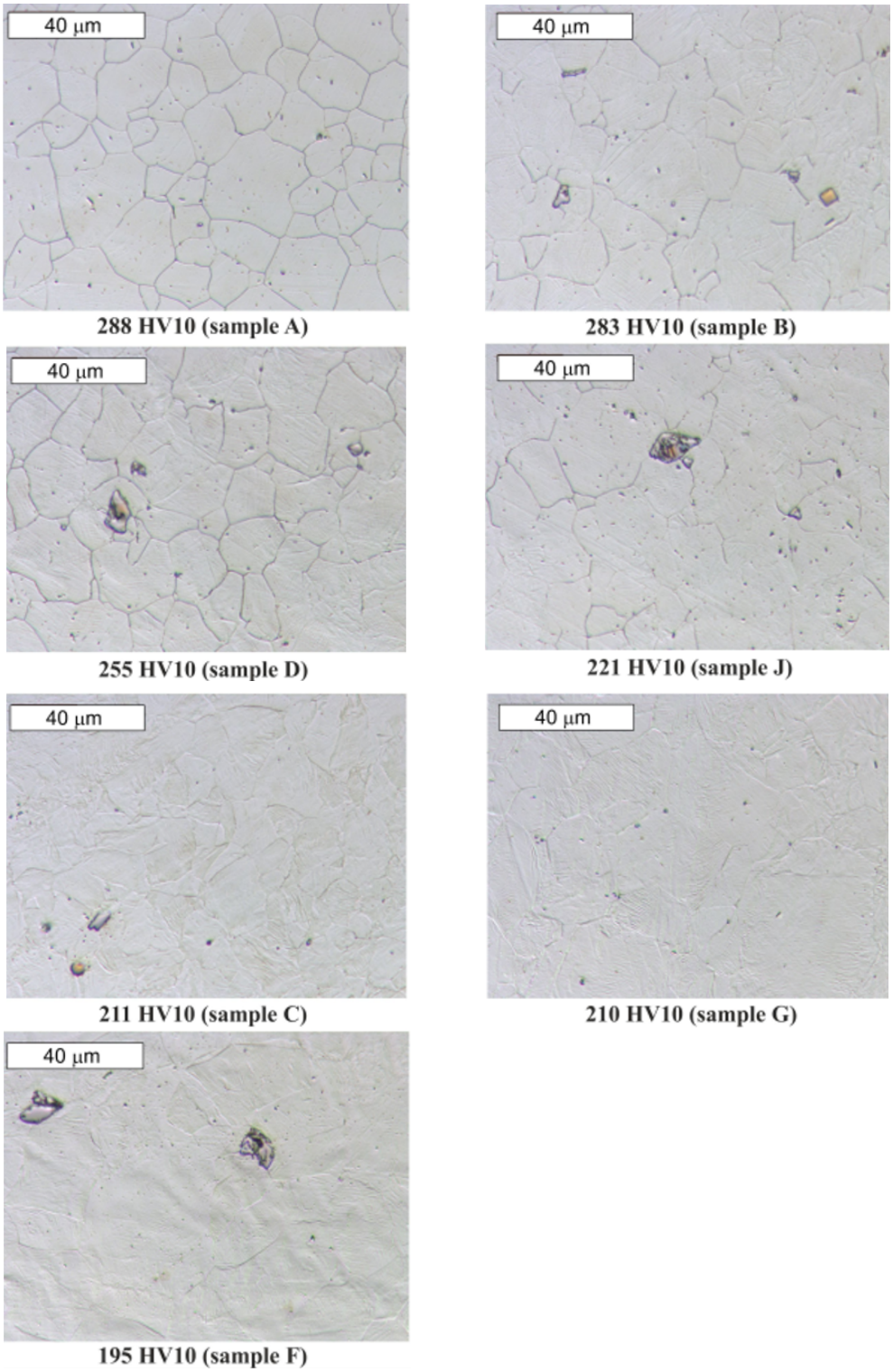

Fig. 13. Microstructure of the other seven preforms according to the decreasing hardness values. Light microscopy, etched

4±0,1 mm and length 30±0,1 mm). The samples were heated to 1050°C at the rate of 5°C/min and cooled at the same rate to about 200°C. Fig. 14 shows the base line as well as the first derivative, which were obtained as a result of the performed thermal analysis. Taking into consideration the analyzed issue, the curves obtained during the heating are important. The diagram course makes it possible to state that, during the heating and the cooling, we observe transformations which can be combined with the dissolution and the precipitation, respectively, of the phases observed on the grain boundaries. It is worth pointing out that, in this alloy, no other transformations occur which could result in analogical changes in the course of the dilatometric curves. The matrix phase remains austenite at temperatures throughout the analyzed range, the observed peaks must be related to the phase evolution within the austenitic matrix. The inititation of the dissolution of these phases takes place during the heating of

the alloy at 702.1°C, and the process lasts until the temperature of 921.9°C is reached. This means that, at the temperature to which the charge material is heated, we should observe dissolution of the phases present on the boundaries of the austenite grains. Mainly carbides of the MC, M_6C and $M_{23}C_6$ type can be formed in Ni-Cr-Fe alloys [17]. Research suggests higher decomposition temperature of the M_7C_3 carbide compared to the $M_{23}C_6$ carbide [43]. For this reason, it should be noted that the precipitates are probably M236 type carbides. The diffusive nature of the carbide dissolution process explains the significance of the heating temperature, holding time and heating rate on the kinetics of the dissolution process. It should be noted that this process takes place in a wide temperature scope, and the the most intensive dissolution occurs at high temperatures. Kostoj et al. [44] were also found that the size of the carbides also influences the rate of transformation. Each temperature fluctuation taking place during the heating leading to charge material inderheating, especially in the case when it is accompanied by its rapid heating, can casue incomplete dissolution of these precipitates. We should also remember that the final temperature of their dissolution can also be affected by the occurring variations of its chemical composition. Kegg et al. [45] found that increasing the nickel content facilitates the nucleation of $M_{23}C_6$ type carbides. Taking into consideration the temperature scope of the forming phases, the latter are probably formed by chromium carbide precipitates. We should, however, not exclude the possibility that they are constituted by precipitates of the sigma phase, which is favoured by a high chromium content in the steel, and which can also precipitate on the grain boundaries [21,22].

On the basis of the obtained diagram, we can also state that, during the cooling of the alloy, the precipitation temperature of these phases is lower and equals 850.5°C. This process lasts until the temperature of 618.2°C is reached, were the most intensive stage is observed also at high tenperatures.

3.5. Results of modelling of the Nireva heating process

Also performed was a numerical simulation of the process of heating and annealing of the NCF3015 material. The presented diagram (Fig. 15) shows the dependence of the temperature on the inductor length, which equals the time of the charge material being present in the coil. The presented curves were determined for the surface layer and the bearing roller core. We can clearly see that the temperature for the bearing roller surface reaches the predetermined temperature, i.e. 1050°C after covering 0,8 m of the inductor length. In turn, for the core, this distance is 1.1 m of the inductor length. The distance for which the surface layer and the bearing roller core are at similar temperatures equals 0.2 m. At this time, we observe microstructure homogenization and proper preparation of the charge material for the extrusion process, thus ensuring repeatability of the microstructure and the hardness in the production process, as well as an increase of the tool durability in the extrusion process. With the introduction of a longer inductor into the process without a change in the time of the charge material feed time, the time of the charge material's presence in the inductor will be prolonged by about 90 seconds.

4. Summary

The performed complex analysis of the wear of forming tools in the process of producing an engine valve forging made it possible to determine the causes of their lower durability resulting from insufficient dissolution of the hard carbide precipitates during the heating of the charge material.

The wear analysis was aided with numerical simulations of the examined forging process, which showed that, for higher charge material temperatures, the normal stress distribution is higher by 400 MPa than in the case of a material with a lower

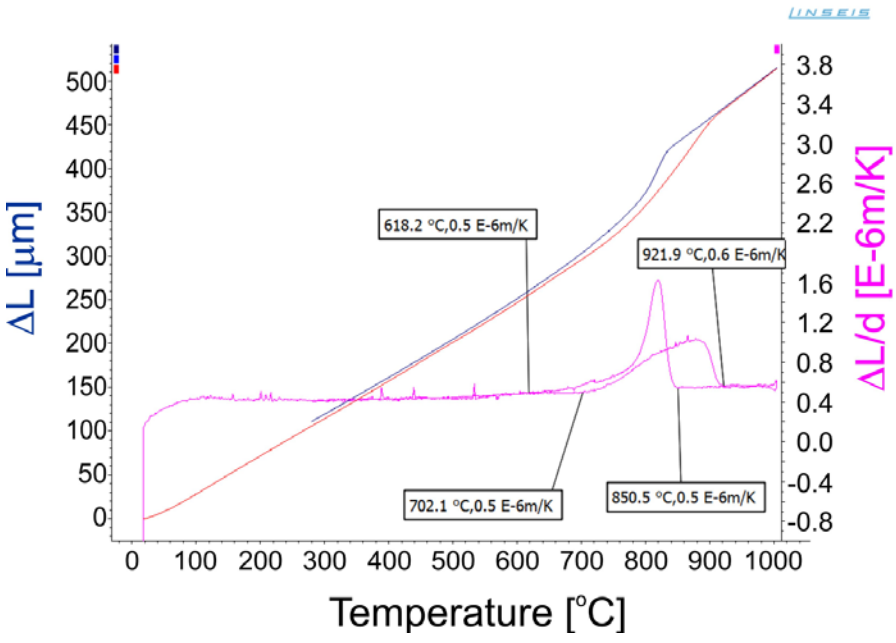

Fig. 14. Dilatometric curves for Nireva

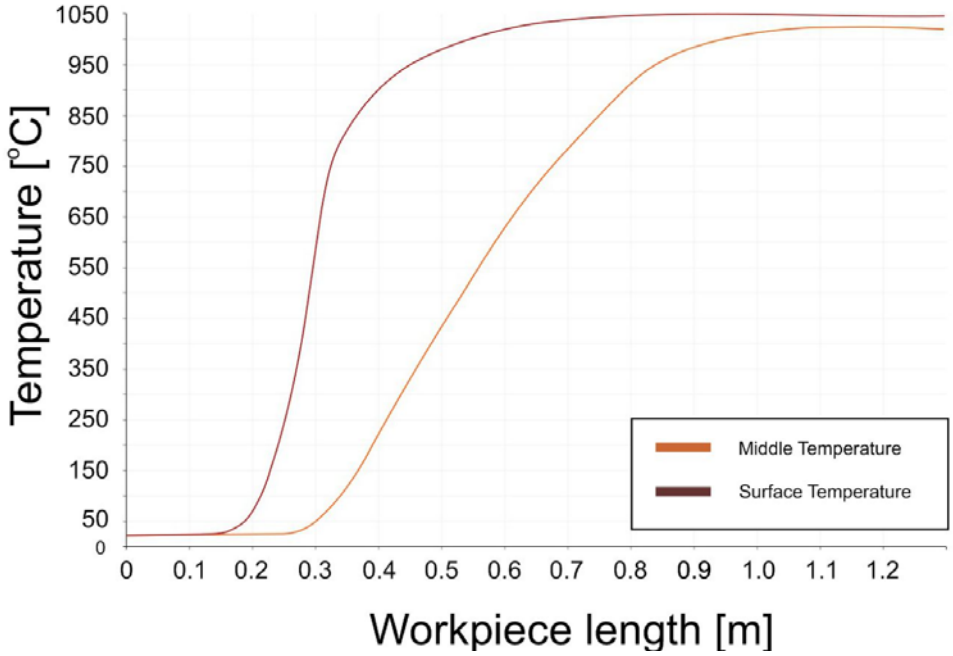

Fig. 15. Dependence of the Nireva temperature on the inductor length made with the use of a numerical simulation program

hardness. Very big differences were also observed for the abrasive wear distribution, where, on the tool for the charge material with a lower temperature in the intermediate zone, the abrasive wear equaled over 4500 MPa. This is analogical to the increase of the extrusion force by 100 kN for the charge material extruded from lower temperatures. The increase in the measured values of stresses, unit pressures and extrusion force on the tool, during the forming of a forging with higher hardness, is the cause of premature tool wear, especially in the cylindrical zone as well as in the area of the forging section reduction field.

The microstructural tests demonstrated that the amount of the dissolved carbides, nitrides and intermetallic phases is in a strong correlation with the hardness of the charge material. The larger amount of carbides on the grain boundaries, the higher the charge material hardness. A worrying fact was the lack of repeatability of the charge material heating process, as the consecutively collected forgings after the heating process differed in the amount of dissolved carbides in the microstructure as well as hardness, which equaled from over 300 HV to 192 HV. At the same time, the lack of repeatability after the heating process directly translates to the tool durability in the extrusion process.

The performed dilatometric tests demonstrated that the phase precipitates present on the grain boundaries can occur up to the temperature of 922°C. We should, however, remember that the temperature and rate of the transformation is strongly connected with the intensity of the heating. With an increase in the heating rate, the transformation time will be shorter, but, at the same time, it will begin at higher temperatures, as the driving force of the transformation will be the increasing difference in the free energy in respect of the equilibrium state. For this reason, we should expect that, with the rapid heating typical of induction heating, the temperature of the final dissolution of these phases will be higher. This, in combination with the cyclic changeability of the heating process, contributed to selective underheating of the preforms at the production stage.

The results of numerical modelling of the charge material heating process showed that the time needed to homogenize the core's microstructure is much longer than in the case of the charge material edges. The longer heating and annealing time of the charge material will provide the possibility to shorten the time of the production cycle and thus also increase the processes efficiency and shorten the time of the forging's contact with the tool, which directly translates to increased tool durability.

REFERENCES

[1] P. Forsberg, P. Hollman, S. Jacobson, Wear **271** (9-10), 2477-2484 (2011). DOI: https://doi.org/10.1016/j.wear.2010.11.039

[2] R. Elo, J. Heinrichs, S. Jacobson, Wear **376-377**, 1429-1436 (2017). DOI: https://doi.org/10.1016/j.wear.2016.12.060

[3] M. Priest, C.M. Taylor, Wear **241**, 193-203, (2000). DOI: https://doi.org/10.1016/S0043-1648(00)00375-6

[4] H. Jeong, J. Choa, H. Park, Journal of Materials Processing Technology **162-163**, 504-511 (2005). DOI: https://doi.org/10.1016/j.jmatprotec.2005.02.101

[5] J. Hongchao, L. Jinping, W. Baoyu, F. Xiaobin, X. Wenchao, H. Zhenghuan, Journal of Materials Processing Technology **240**, 1-11 (2017). DOI: https://doi.org/10.1016/j.jmatprotec.2016.09.004

[6] H. Morii, H. Yoshimura. US Patent No. 8881391 B2. (2014).

[7] Z. Yuanzhia, Y. Zhimin, X. Jiangpin, Journal of Alloys and Compounds **509** (20), 6106-6112 (2011). DOI: https://doi.org/10.1016/j.jallcom.2011.03.038

[8] H.S. Jeong, J.R. Choa, H.C. Park, J. Mater. Process. Technol. **162-163**, 504-511 (2005). DOI: https://doi.org/10.1016/j.jmatprotec.2005.02.101

[9] D.K. Kim, D.Y. Kim, S.H. Ryu, D.J. Kim, J. Mater. Process. Technol. **113** (1-3), 148-152 (2001). DOI: https://doi.org/10.1016/S0924-0136(01)00700-2

[10] B. Painter, R. Shivpuri, T. Altan, J. Mater. Process. Technol. **59**, 132-143 (1996). DOI: https://doi.org/10.1016/0924-0136(96)02294-7

[11] H.M. Tawancy, Journal of Materials Science **41** (24), (2006). DOI: https://doi.org/10.1007/s10853-006-0990-y

[12] P.E.A. Turchi, L. Kaufman, Z.-K. Liu, Calphad **30** (1), 70-87 (2006). DOI: https://doi.org/10.1016/j.calphad.2005.10.003

[13] Y.L. Lu, L.M. Pike, C.R. Brooks P.K. Liaw, D. Klarstrom, Scripta Materialia **56** (2), 121-124 (2007). DOI: https://doi.org/10.1016/j.scriptamat.2006.09.011

[14] A. Ul-Hamid, A.I. Mohammed, S.S. Al-Jaroudi, H.M. Tawancy, N.M. Abbas, Materials Characterization **58** (1), 13-23 (2007). DOI: https://doi.org/10.1016/j.matchar.2006.03.005

[15] F. Bayata, A.T. Alpas. Wear, **480-481**, 203943 (2021). DOI: https://doi.org/10.1016/j.wear.2021.203943

[16] Z. Shen, J. Zhang, S. Wu, X. Luo, B.M. Jenkins, M.P. Moody, S. Lozano-Perez, X. Zeng, Acta Materialia **226**, 117634 (2022). DOI: https://doi.org/10.1016/j.actamat.2022.117634

[17] M. Knyazeva, M. Pohl, Metallography, Microstructure and Analysis **2** (5), 343-351 (2013). DOI: https://doi.org/10.1007/s13632-013-0088-2

[18] S.S. Hwang, Y.S. Lim, S.W. Kim, D.J. Kim, H.P. Kim, Nuclear Engineering and Technology **45** (1), 73-80 (2013). DOI: http://dx.doi.org/10.5516/NET.07.2012.013

[19] L.J. Wang, L.Y. Sheng, C.M. Hong, Materials & Design **37**, 349-355 (2012). DOI: https://doi.org/10.1016/j.matdes.2012.01.024

[20] R.B. Frank, Advanced Materials and Processes **163** (6), 37-42 (2005).

[21] Ch. Hsieh, W. Wu, ISRN Metallurgy **2012** (1), 732471 (2012). DOI: https://doi.org/10.5402/2012/732471

[22] G. Golański, M.M. Lachowicz, Engineering Failure Analysis **105**, 490-495 (2019). DOI: https://doi.org/10.1016/j.engfailanal.2019.07.024

[23] J. Zhou, Z. Sun, P. Kanout'e, D. Retraint, International Journal of Fatigue **103**, 309-317 (2017). DOI: https://doi.org/10.1016/j.ijfatigue.2017.06.011

[24] R. Elo, J. Heinrichs, S. Jacobson, Wear **376-377** (Part B), 1429-1436, (2017). DOI: https://doi.org/10.1016/j.wear.2016.12.060

[25] A. Mühlbauer, History of Induction Heating and Melting, Vulkan-Verlag GmbH, Essen (2008).

[26] O. Lucía, P. Maussion, E.J. Dede, J.M. Burdío, IEEE Trans. Ind. Electron **61** (5), 2509-2520 (2014). DOI: https://doi.org/10.1109/TIE.2013.2281162

[27] J. Egalon, S. Caux, P. Maussion, M. Souley, O. Pateau, IEEE Transactions on Industry Applications **48** (5), 1692-1699 (2012). DOI: https://doi.org/ 10.1109/TIA.2012.2210176

[28] Z. Xiang, B. Ducharne, N.D. Schiava, J.F. Capsal, P.J. Cottinet, G. Coativy, P. Lermusiaux, M.Q.Q. Le, Materials and Design **174**, 107804 (2019). DOI: https://doi.org/10.1016/j.matdes.2019.107804

[29] M.E. Cano, A. Barrera, J.C. Estrada, A. Hernandez, T. Cordova, Review of Scientific Instruments **82** (11), 114904 (2011). DOI: https://doi.org/10.1063/1.3658818

[30] B.J. Yang, A. Hattiangadi, W.Z. Li, G.F. Zhou, T.E. McGreevy, Materials Science and Engineering A **527** (12), 2978-2984 (2010). DOI: https://doi.org/10.1016/j.msea.2010.01.038

[31] E. Summerville, K. Venkatesan, C, Subramanian, Material and Design **16** (5), 289-294 (1995). DOI: https://doi.org/10.1016/0261-3069(96)00010-6

[32] O. Barrau, C. Boher, R. Gras, F. Rezai-Aria, Wear **255** (7-12), 1444-1454 (2003). DOI: https://doi.org/10.1016/S0043-1648(03)00280-1

[33] M. Hawryluk, J. Ziemba, M. Zwierzchowski, M. Janik, Wear **476**, 203749 (2021). DOI: https://doi.org/10.1016/j.wear.2021.203749

[34] M. Hawryluk, M. M. Lachowicz, M. Janik, J. Ziemba, Z. Gronostajski, Archives of Civil and Mechanical Engineering **21** (151), 1-17 (2021). DOI: https://doi.org/10.1007/s43452-021-00301-8

[35] M. Hawryluk, Z. Gronostajski, M. Kaszuba, J. Krawczyk, P. Widomski, J. Ziemba, M. Zwierzchowski, M. Janik, Archives of Metallurgy and Materials **63** (4), 1963-1974 (2018). DOI: https://doi.org/10.24425/amm.2018.125131

[36] H.S. Jeong, J.R. Cho, H.C. Park, Journal of Materials Processing Technology **162-163**, 504-511 (2005). DOI: https://doi.org/10.1016/j.jmatprotec.2005.02.101

[37] T.M. Ivansju, J. Epp, H.W. Zoch, A. de Silva Rocha, Materials Research **22** (5), (2019). DOI: https://doi.org/10.1590/1980-5373-MR-2019-0230

[38] Y.C. Lin, M.S. Chen, J. Zhong, Computational Materials Science **43** (4), 1117-1122 (2008). DOI: https://doi.org/10.1016/j.commatsci.2008.03.010

[39] A. Polkowska, S. Lech, P. Bała, W. Polkowski, Materials Characterization **171**, 110737 (2021). DOI: https://doi.org/10.1016/j.matchar.2020.110737

[40] L.J. Wang, L.Y. Sheng, C.M. Hong, Materials & Design **37**, 349-355 (2012). DOI: https://doi.org/10.1016/j.matdes.2012.01.024

[41] Y. Li, Y. Gao, B. Xiao, T. Min, Y. Yang, S. Ma, D. Yi, Journal of Alloys and Compounds **509** (17), 5242-5249 (2011). DOI: https://doi.org/10.1016/j.jallcom.2011.02.009

[42] K. Wieczerzak, P. Bala, R. Dziurka, T. Tokarski, G. Cios, T. Kozel, L. Gondek, Journal of Alloys and Compounds **698**, 673-684 (2017). DOI: https://doi.org/10.1016/j.jallcom.2016.12.252

[43] R. Rahimi, O. Volkova, H. Biermann, J. Mola, Advanced Engineering Materials **21** (5), (2018). DOI: https://doi.org/10.1002/adem.201800658

[44] V. Kostoj, J.D. Mithieux, T. Fröhlich, Solid State Phenomena **172-174**, 426-431 (2011). DOI: https://doi.org/10.4028/www.scientific.net/SSP.172-174.426

[45] G.R. Kegg, J.M. Silcock, Metal Science Journal **6** (1), 47-56 (2013). DOI: https://doi.org/10.1179/030634572790445966